for conversion to the pyrophosphate is postulated. This involves loss of the bridging H_2O molecule with movement of the resulting square pyramids around the edge-shared "hinge" to a position where vanadyl groups are parallel. Half of the vanadyl oxygen atoms are slightly shifted, giving rise to the edge-shared octahedral arrangement where the octahedral dimers have vanadyl bonds pointing in opposite directions.[2] After proton migration, half of the phosphate tetrahedra each lose an apical oxygen atom in the form of an H_2O molecule. These coordinately unsaturated PO_3 units invert and interact with PO_4 tetrahedra above or below to form pyrophosphate groups. This mechanism leaves all V–O–P connections intact and involves primarily the breaking of weak V–OH_2 and P–OH_2 bonds. Although a structural change occurs on an atomic level, no change in particle morphology was observed in scanning electron micrographs taken before and after the structural conversion.

Acknowledgment. The authors thank R. Jakeman for valuable discussions and M. Sweeten for technical assistance.

Registry No. $(VO)_2H_4P_2O_9$, 89415-02-1.

Supplementary Material Available: Listings of positional and thermal parameters and interatomic distances (2 pages). Ordering information is given on any current masthead page.

(6) Contribution No. 3424.

Central Research and Development Department[6]
E. I. du Pont de Nemours and Company
Experimental Station
Wilmington, Delaware 19898

C. C. Torardi*
J. C. Calabrese

Received January 9, 1984

Articles

Contribution from the Chemistry Department, University of Tasmania, Hobart, Tasmania 7001, Australia, and Institut für Physikalische Chemie, Westfälische Wilhems-Universitat, Münster D-4400, West Germany

EPR and Optical Spectra of $CuCl_4^{2-}$ Doped into Single Crystals of Several Zinc(II) Host Lattices

ROBERT J. DEETH,† MICHAEL A. HITCHMAN,*† GERHARD LEHMANN,‡ and HUBERT SACHS‡

Received June 1, 1983

The EPR and electronic spectra of copper-doped diethylenediammonium hexachlorozincate(II), $(enH_2)_2Zn[Cu]Cl_6$, cesium tetrachlorozincate(II), and rubidium tetrachlorozincate(II) are reported and in each case suggest the presence of distorted-tetrahedral $CuCl_4^{2-}$ ions. At 77 K the EPR spectrum of $(enH_2)_2Zn[Cu]Cl_6$ exhibits both copper hyperfine and chlorine superhyperfine structure. As with other pseudotetrahedral copper(II) complexes the hyperfine parameters cannot be explained satisfactorily from the simple equations generally used for planar and distorted-octahedral complexes. The principal axis of each superhyperfine tensor apparently deviates significantly from the chlorine–copper bond direction, and it is suggested that this is probably because the ligands do not lie along the molecular x and y axes. The molecular **g** tensor of $(enH_2)_2Zn[Cu]Cl_6$ is highly rhombic, with the d_{z^2} orbital making a significant contribution to the metal part of the ground-state wave function. Angular-overlap calculations suggest that the rhombic perturbation to the ligand field in this compound is caused by a substantial difference between the angles subtended by the chlorine ligands at the copper ion, and the distortions estimated for the $CuCl_4^{2-}$ ions present in all three complexes are interpreted in terms of Jahn–Teller and lattice-induced perturbations.

Introduction

The compounds of copper(II) exhibit an unusually wide range of stereochemistries.[1] Moreover, these complexes tend to be quite plastic:[2] that is, they can often be readily deformed so that factors such as crystal packing and hydrogen bonding may strongly influence the geometry of any particular molecule. This is the case, for instance, for the $CuCl_4^{2-}$ ion, which exhibits a stereochemistry ranging from near-tetrahedral in $((CH_3)_3NH)_3Cu_2Cl_7$[3] to square planar in, for instance, $[C_6H_5C_2H_4N(CH_3)H_2]CuCl_4$.[4] There are many examples of intermediate geometries, with the majority of tetrachlorocuprates having a flattened tetrahedral ligand arrangement of approximately D_{2d} symmetry.[5] The stereochemistry of copper(II) complexes is thought to be strongly influenced by the Jahn–Teller effect, which predicts that a regular tetrahedral geometry should be unstable. Qualitatively, the geometries observed for the $CuCl_4^{2-}$ ion may be rationalized in terms of a distortion along one component of the active Jahn–Teller mode of E symmetry,[6] with the final structure being determined by a balance between the ligand field stabilization of the square-planar geometry and the destabilizing effect of ligand–ligand repulsions.

Because of its relative simplicity and wide range of stereochemistries, the electronic structure of the $CuCl_4^{2-}$ ion has been the subject of numerous theoretical studies, from detailed molecular orbital calculations[7,8] through simple angular-overlap[9–11] and crystal field[12] calculations. Experimentally,

† University of Tasmania.
‡ Westfälische Wilhems-Universitat.

(1) Hathaway, B. J.; Billing, D. E. *Coord. Chem. Rev.* **1970**, *5*, 43. Hathaway, B. J. *Struct. Bonding (Berlin) 14*, **1973**, 49.
(2) Gays, J.; Bersuker, I. B.; Garaj, J.; Kabesova, M.; Kohout, J.; Langfelderova, H.; Melrick, M.; Serator, M.; Valach, F. *Coord. Chem. Rev.* **1976**, *19*, 253. Hathaway, B. J. *Ibid.* **1981**, *35*, 211.
(3) Clay, R. M.; Murray-Rust, P.; Murray-Rust, J. *J. Chem. Soc., Dalton Trans.* **1973**, 593.
(4) Harlow, R. L.; Wells, W. J., III; Watt, G. W.; Simonsen, S. H. *Inorg. Chem.* **1974**, *13*, 2106.
(5) For a review of all aspects of chlorocuprate chemistry see: Smith, D. W. *Coord. Chem. Rev.* **1976**, *21*, 93.
(6) Bacci, M. *Chem. Phys.* **1979**, *40*, 237.
(7) Ros, P.; Shuit, G. C. G. *Theor. Chim. Acta* **1966**, *4*, 1.
(8) Demuynck, J.; Veillard, A.; Wahlgren, U. *J. Am. Chem. Soc.* **1973**, *95*, 5563.
(9) Day, P.; Jørgensen, C. K. *J. Chem. Soc.* **1964**, 6226.

0020-1669/84/1323-1310$01.50/0

these models have been tested by the complementary techniques of EPR and electronic spectroscopy, the former focusing attention on the ground state and the latter on excited-state properties. The most detailed studies have been carried out on copper-doped cesium tetrachlorozincate, $Cs_2Zn[Cu]Cl_4$, the electronic spectrum having been reported by Ferguson[13] and the EPR and electronic spectra by Sharnoff and co-workers.[14,15] The latter workers concluded that the g and metal hyperfine parameters suggest a significant admixture of the metal 4p orbitals in the ground-state wave function. In particular, A_z was observed to be anomalously small in magnitude,[15] and it has subsequently been found[16] that this is a general property of copper(II) complexes in a pseudotetrahedral ligand environment. A similar characteristic has been observed for the so-called copper blue proteins,[17] which are now known to involve copper(II) ions in a highly distorted-tetrahedral ligand environment.[18]

In the above studies of $Cs_2Zn[Cu]Cl_4$,[13-15] as in most earlier work of this kind, the diamagnetic host lattice was merely considered to provide a matrix to hold the $CuCl_4^{2-}$ ion in a fixed orientation in space, with the guest being assumed to adopt a geometry similar to that of the pure copper(II) compounds. More recently, it has been recognized that in doping experiments of this kind the host lattice may induce distortions upon the guest complex and that these may in fact provide information on the balance between electronic and steric forces that decide the equilibrium nuclear geometry of the copper compound.[2,19,20] Recently, Lehmann and co-workers have reported[21-23] the effects of such lattice perturbations on the EPR spectrum of Mn^{2+} doped into single crystals of a number of complexes containing $ZnCl_4^{2-}$ and $ZnBr_4^{2-}$ ions having varying degrees of distortion away from a regular-tetrahedral geometry. We have since extended these studies by measuring the EPR and optical spectra of Cu^{2+} doped into single crystals of several of the zinc(II) chloro complexes, and the results are presented in the present paper. The electronic structures and probable geometries of the copper(II) complexes have been deduced and interpreted in terms of a balance between lattice effects and the "preferred" stereochemistry of the free $CuCl_4^{2-}$ ion. In addition, in one case, hyperfine and superhyperfine coupling with the copper and chlorine nuclei was observed in the EPR spectrum, allowing a quite detailed analysis of the unpaired electron density in the complex.

Experimental Section

Preparation of the Compounds. Large, well-formed, pale yellow crystals of copper-doped diethylenediammonium hexachlorozincate(II), $(enH_2)_2Zn[Cu]Cl_6$, cesium tetrachlorozincate(II), $Cs_2Zn[Cu]Cl_4$, and rubidium tetrachlorozincate(II), $Rb_2Zn[Cu]Cl_4$, were prepared by allowing stoichiometric amounts of the reagents dissolved in dilute hydrochloric acid to evaporate slowly at room temperature, with 5 mol % of the zinc chloride replaced by copper chloride. Analysis of

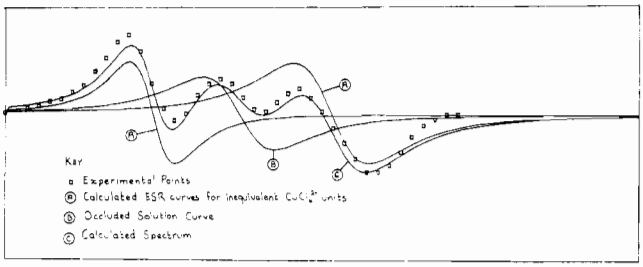

Figure 1. Computer simulation of the EPR spectrum of $Cs_2Zn[Cu]Cl_4$ in terms of three Lorenzian lines.

$Rb_2Zn[Cu]Cl_4$ (by atomic absorption spectroscopy) suggested that this contains 2.0 mol % copper(II), and a comparison of the integrated EPR signal intensities at 103 K suggested concentrations of ~0.15 and ~0.05 mol % of copper(II) in $(enH_2)_2Zn[Cu]Cl_6$ and $Cs_2Zn[Cu]Cl_4$, respectively. A sample of the ethylenediammonium salt in which the amine protons were largely replaced by deuterium atoms, $(enD_2)_2Zn[Cu]Cl_6$, was prepared by dissolving 100 mg of $(enH_2)_2Zn[Cu]Cl_6$ in 50 mL of D_2O containing 3 drops of concentrated hydrochloric acid and allowing the resulting solution to evaporate to dryness.

EPR Spectra. Measurements were made on a JEOL JES FE3x spectrometer operating at X-band frequency. A variable-temperature accessory allowed measurements down to 103 K, and an insertion Dewar was used to obtain spectra at 77 K. Single-crystal measurements were made as described previously[24] for rotations about the three orthogonal crystal axes for each of the complexes $(enH_2)_2Zn[Cu]Cl_6$, $Cs_2Zn[Cu]Cl_4$, and $Rb_2Zn[Cu]Cl_4$, these being carried out by using a JEOL rotation accessory. The crystal morphologies were deduced with use of a polarizing microscope, and this was also used to align the crystals with respect to the rotation axis. Each crystal was mounted at least twice for every rotation to minimize errors in alignment. For each compound the room-temperature spectra showed relatively broad, weak signals. On cooling to 103 K, the signals sharpened markedly, without showing any significant change in position, and the measurements at this temperature were used to derive the molecular g values of the complexes. The spectra were calibrated by using a spectrum of powdered α,α'-diphenyl-β-picrylhydrazyl (DPPH), $g = 2.0036$, placed close to the crystal.

The compounds exhibited qualitatively similar trends in their EPR spectra. For two rotations, a single symmetric peak was observed, which reached its maximum and minimum shift from DPPH when the external magnetic field was along a crystal axis. In the third rotation a single symmetric signal was observed only when the external field was along a crystal axis; for all other orientations two signals of half the intensity of the single resonance were observed. The reason for this behavior becomes apparent when the orientation of the molecular **g** tensors in each crystal lattice is considered (see below). For $(enH_2)_2Zn[Cu]Cl_6$ the two signals were generally well resolved, whereas for $Cs_2Zn[Cu]Cl_4$ and $Rb_2Zn[Cu]Cl_4$ they were not. Moreover, for the latter two complexes, a third peak was apparent in this third rotation. It was found that the spectra could be satisfactorily resolved into the derivatives of three Lorentzian curves (see Figure 1), two varying in position according to the orientation of the crystal and the third being reasonably isotropic and constant in intensity for all crystal orientations. This suggests that the third signal is spurious and is due to a small amount of solution included in each crystal. For these two rotations, therefore, the EPR parameters were derived using g values obtained from the "best-fit" Lorenzian analysis of the spectra. While it is thought that this provides reasonable estimates of the molecular g values, the results for these two complexes are considerably less accurate than for $(enH_2)_2Zn[Cu]Cl_6$. Typical spectra for various crystal orientations of the compounds are shown in Figure 2, while the g values plotted as a function of the rotation angles are given in Figure 3. The measured g values are reported as supplementary material.

Electronic Spectra. The electronic spectra of the (010) and (112) crystal faces of $(enH_2)_2Zn[Cu]Cl_6$ and the (010) crystal face of $Cs_2Zn[Cu]Cl_4$ were measured at room temperature and 8 K over the range 2500–330 nm with the electric vector of polarized light parallel to the extinction directions of each crystal face. The crystals were

(10) Smith, D. W. *J. Chem. Soc. A* **1969**, 2529; **1970**, 2900.
(11) Hitchman, M. A.; Cassidy, P. *Inorg. Chem.* **1978**, *17*, 1682.
(12) Gerloch, M.; Slade, R. C. "Ligand Field Parameters"; Cambridge University Press: New York, 1973.
(13) Ferguson, J. *J. Chem. Phys.* **1964**, *40*, 3406.
(14) Sharnoff, M.; Reimann, C. *J. Chem. Phys.* **1965**, *43*, 2993.
(15) Sharnoff, M. *J. Chem. Phys.* **1965**, *42*, 3383.
(16) Yokoi, H.; Addison, A. W. *Inorg. Chem.* **1977**, *16*, 1341.
(17) Fee, J. A. *Struct. Bonding (Berlin)* **1975**, *23*, 1.
(18) Colman, P. J.; Freeman, H. C.; Guss, J. M.; Murata, M.; Norris, V. A.; Ramshaw, J. A. M.; Venkatappa, M. P. *Nature (London)* **1978**, *272*, 319.
(19) Hathaway, B.: Duggan, M.; Murphy, A.; Mullane, J.; Power, C.; Walsh, A.; Walsh, B. *Coord. Chem. Rev.* **1981**, *36*, 267.
(20) Reinen, D.; Krause, S. *Inorg. Chem.* **1981**, *20*, 2750.
(21) Sachs, H.; Lehmann, G. *Phys. Status Solidi. B* **1979**, *92*, 417.
(22) Lehmann, G. *Phys. Status Solidi B* **1980**, *99*, 623.
(23) Heming, M.; Lehmann, G.; Henkel, G.; Krebs, B. *Z. Naturforsch., A* **1981**, *36A*, 286.
(24) Waite, T. D.; Hitchman, M. A. *Inorg. Chem.* **1976**, *15*, 2155.

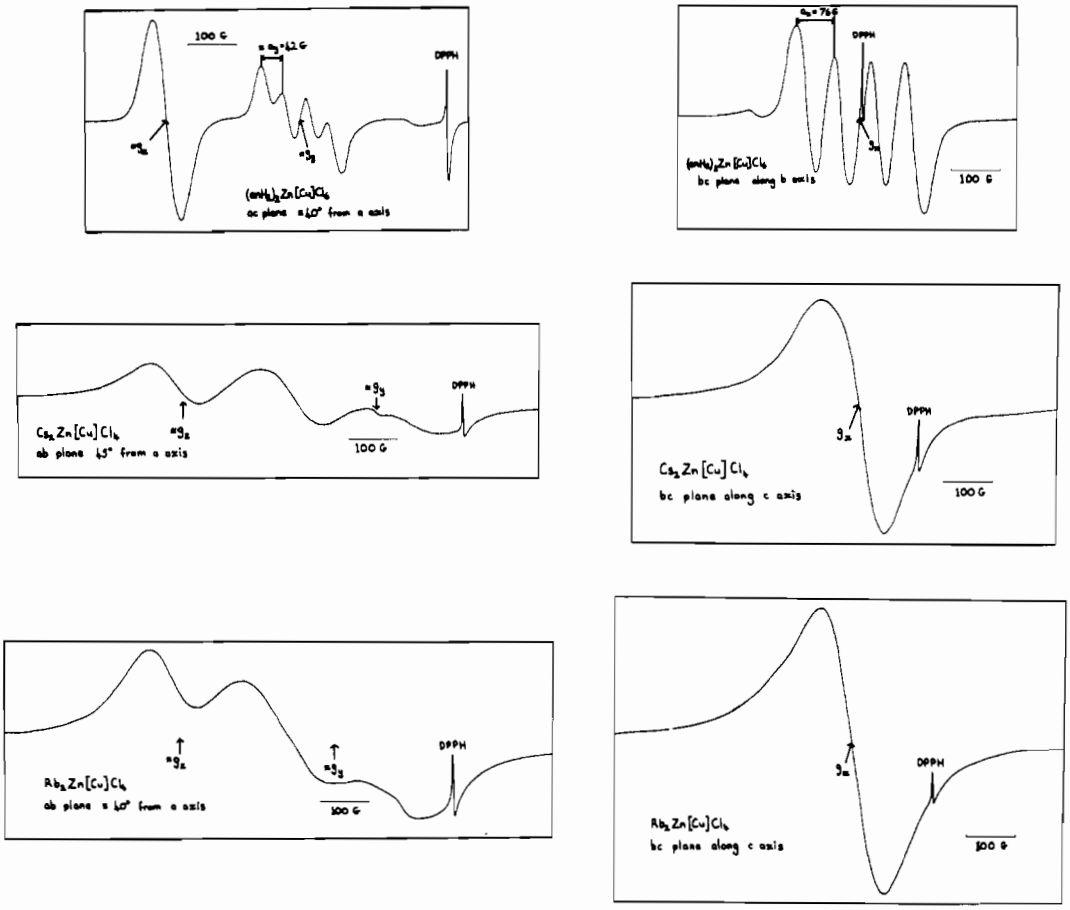

Figure 2. Typical EPR spectra of $(enH_2)_2Zn[Cu]Cl_6$, $Cs_2Zn[Cu]Cl_4$, and $Rb_2Zn[Cu]Cl_4$ for various crystal orientations.

Table I. Space Group, Unit Cell Dimensions (Å), and Important Bond Distances (Å) and Angles (deg) for $(enH_2)_2ZnCl_6$, Cs_2ZnCl_4, and Rb_2ZnCl_4

	$(enH_2)_2ZnCl_6$[a]	Cs_2ZnCl_4[b]	Rb_2ZnCl_4[c]
space group	*Pnma*	*Pnma*	*Pnma*
a	12.923	9.737	9.2636
b	19.291	12.972	7.2859
c	6.187	7.392	12.7193
Zn-Cl(1)	2.285	2.249	2.233
Zn-Cl(2)	2.326	2.259	2.254
Zn-Cl(3,3′)	2.260	2.252	2.241
Cl(3)-Zn-Cl(3′)	125.43	109.03	107.3
Cl(1)-Zn-Cl(2)	107.52	115.34	114.3

[a] Reference 26. [b] Reference 29. [c] Reference 25.

Table II. Selection Rules for $[CuCl_4]^{2-}$ in the C_{2v} and D_{2d} Point Groups

C_{2v}		D_{2d}	
transition	mol polarizn axis	transition	mol polarizn axis
$^2A_1(d_{z^2}) \leftarrow {}^2A_1(d_{x^2-y^2})$	z	$^2A_1(d_{z^2}) \leftarrow {}^2B_2(d_{xy})$	z
$^2A_2(d_{xy}) \leftarrow {}^2A_1(d_{x^2-y^2})$	...	$^2B_1(d_{x^2-y^2}) \leftarrow {}^2B_2(d_{xy})$	...
$^2B_1(d_{xz}) \leftarrow {}^2A_1(d_{x^2-y^2})$	x	$^2E(d_{xz},d_{yz}) \leftarrow {}^2B_2(d_{xy})$	x, y
$^2B_2(d_{yz}) \leftarrow {}^2A_1(d_{x^2-y^2})$	y		

mounted on copper masks, and the spectra were recorded on a Cary 17 spectrophotometer, the samples being cooled using a Cryodyne Model 21 cryostat. Typical spectra at 8 K are shown in Figure 4, the only significant effect accompanying cooling being a sharpening of each band. Reflectance spectra of powders of the complexes were measured at room temperature by using a Beckman DK2A spectrophotometer.

Results and Discussion

Crystallography and Molecular Coordinate System of the Zinc(II) Complexes. The crystal structures of Rb_2ZnCl_4,[25] Cs_2ZnCl_4,[29] and $(enH_2)_2ZnCl_6$[26] have been accurately solved. Each compound contains discrete, distorted-tetrahedral $ZnCl_4^{2-}$ units. The space groups, unit cell dimensions, and important bond distances and angles of the MCl_4^{2-} groups are given in Table I. It is apparent that each MCl_4^{2-} ion can be described in terms of the idealized geometry indicated in Figure 5, with the main deviations from a regular T_d ligand arrangement being assumed to be due to the inequalities in the ∠ClZnCl angles, one, α, being significantly greater than the tetrahedral value and the other, β, being slightly smaller. In Cs_2ZnCl_4 and Rb_2ZnCl_4 the differences in the Zn–Cl bond distances are very small (Table I). The bond length differences in $(enH_2)_2ZnCl_6$ are somewhat larger, but calculations suggest that deviations of this kind should have little effect on the electronic properties of the guest copper(II) complex;[28] this is borne out by the orientation of the principal **g** tensors in the doped systems (see subsequent section). The properties of the guest $CuCl_4^{2-}$ ions have therefore been described by using the coordinate system indicated in Figure 5, with the z axis being defined as the bisector of the angle α, the x axis being orthogonal to z and in the plane containing the atoms defining the angle α, and the y axis being orthogonal to z and x. It

(25) Secco, A. S.; Trotter, J. *Acta Crystallogr. Sect. C: Cryst. Struct. Commun.* **1983**, *C39*, 317.
(26) Haüsler, K. G.; von Schnering, H. G., to be submitted for publication.
(27) Scaife, D. E. *Aust. J. Chem. 24*, **1971**, 1315.
(28) Hitchman, M. A.; Deeth, R. J., unpublished work. Deeth, R. J. Honors Thesis, University of Tasmania, 1981.

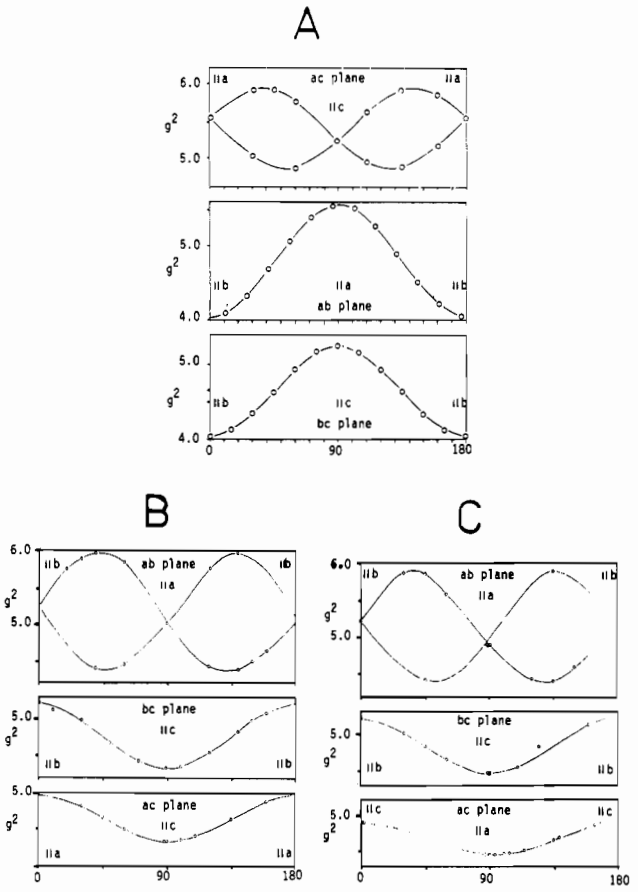

Figure 3. Plots of g^2 vs. angle for crystal rotation: A, $(enH_2)_2Zn[Cu]Cl_6$; B, $Cs_2Zn[Cu]Cl_4$; C, $Rb_2Zn[Cu]Cl_4$.

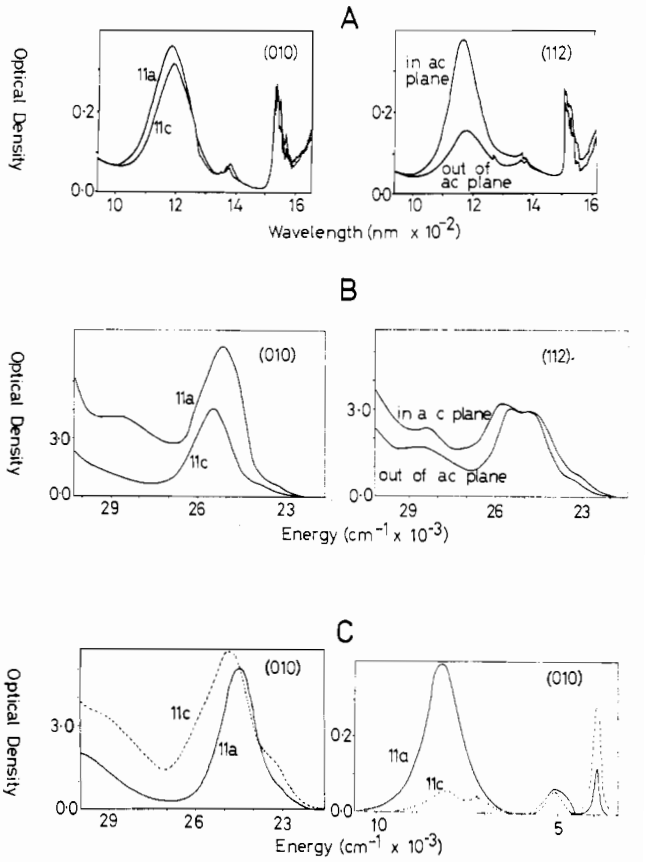

Figure 4. Polarized electronic spectra at 8 K: A, $(enH_2)_2Zn[Cu]Cl_6$; B, $(enH_2)_2Zn[Cu]Cl_6$; C, $Cs_2Zn[Cu]Cl_4$. The crystal planes are indicated in parentheses.

Table III. Molecular Projections for the Polarized Crystal Spectra of $(enH_2)_2Zn[Cu]Cl_6$ and $Cs_2Zn[Cu]Cl_4$

cryst face	polarizn	sq mol projection x^2	y^2	z^2
	$(enH_2)_2Zn[Cu]Cl_6$			
(010)	$\parallel a$	0.00	0.41	0.59
	$\parallel c$	0.00	0.59	0.41
(112)	$\parallel ac$	0.00	0.50	0.50
	$\perp ac$	0.70	0.15	0.15
	$Cs_2Zn[Cu]Cl_4$			
(010)	$\parallel a$	0.44	0.00	0.56
	$\parallel c$	0.00	1.00	0.00

should be noted that in Cs_2CuCl_4 and similar pure copper(II) complexes, $CuCl_4^{2-}$ has a geometry conveniently described in a similar manner, with angles $\alpha \approx \beta \approx 130°$.[29]

Electronic Spectra of the Complexes. "d–d" Transitions (3500–12 000 cm^{-1}). The copper(II) guest complexes are assumed to belong to the pointgroup C_{2v} (Figure 5), the relatively minor deviation from D_{2d} symmetry being due to the inequivalence of the angles α and β. The electric dipole selection rules for the various "d–d" transitions in these two point groups are shown in Table II. All four electronic transitions are observed in the spectrum of the (010) crystal face of $Cs_2Zn[Cu]Cl_4$ (Figure 4C). The band at 8200 cm^{-1} is considerably more intense when the electric vector is parallel to the *a* crystal axis, while that at 3940 cm^{-1} is more intense in *c* polarization. The band at 7210 cm^{-1} occurs weakly in both polarizations. The molecular projections made by a unit vector directed along the two crystal axes are shown in Table III, from which it may be seen that the band at 3940 cm^{-1} is *y* polarized, while that at 8200 cm^{-1} is *x* and/or *z* polarized. This is consistent with the band at 8200 cm^{-1} being due to the transition $^2A_1(d_{x^2-y^2}) \rightarrow {}^2A_1(d_{z^2})$, that at 5050 cm^{-1} to $^2A_1(d_{x^2-y^2}) \rightarrow {}^2B_1(d_{xz})$, and that at 3940 cm^{-1} to $^2A_1(d_{x^2-y^2}) \rightarrow {}^2B_2(d_{yz})$, with the unpolarized weak band at 7210 cm^{-1} being assigned to the formally forbidden transition $^2A_1(d_{x^2-y^2}) \rightarrow {}^2A_2(d_{xy})$. The observed spectrum is quite similar to that reported by Ferguson[13] for copper-doped Cs_2ZnCl_4, and the present assignment is essentially identical with that proposed in the previous work.

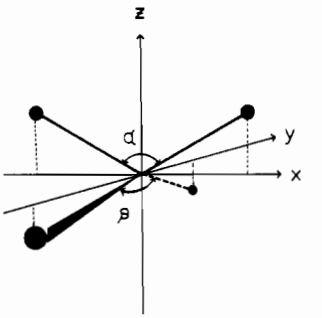

Figure 5. Idealized stereochemistry of the distorted MCl_4^{2-} ion.

The spectra of the (010) and (112) crystal faces of $(enH_2)_2Zn[Cu]Cl_6$ show bands at 8480 and 7800 cm^{-1} with polarization behavior analogous to those of the higher energy bands in $Cs_2Zn[Cu]Cl_4$ (Table IV), so that these may be assigned to the transitions $^2A_1(d_{z^2})$ and $^2A_2(d_{xy}) \leftarrow {}^2A_1(d_{x^2-y^2})$, respectively. The region below 6000 cm^{-1} in this complex is dominated by peaks due to infrared overtones associated with the amine cations, so that the remaining "d–d" transitions could not be resolved in the crystal spectra. A sample in which the amine hydrogen atoms were largely replaced by deuterium was prepared, and although a suitable single crystal for spectral

(29) McGinnity, J. A. *J. Am. Chem. Soc.* **1972**, *94*, 8406; *Inorg. Chem.* **1974**, *13*, 1057.

Table IV. Electronic Transition Energies (cm^{-1}) and Their Assignments[a]

compd	"d-d" region				charge-transfer		
	$^2B_2(d_{yz})$	$^2B_1(d_{xz})$	$^2A_2(d_{xy})$	$^2A_1(d_{z^2})$	$^2A_2$	^2E	$^2B_2$
$(enH_2)_2Zn[Cu]Cl_6$	...	...	7800[b]	8480[b]	23 400[b]	(25 150, 25 600)[b]	28 600[b]
	4420[c]	5360[c]	7700[c]	8950[c]			
$Cs_2Zn[Cu]Cl_4$	3940[b]	5050[b]	7200[b]	8200[b]	23 400[b]	(24 500, 24 800)[b]	29 000[b]
	4250[c]	4560[c]	7330[c]	8260[c]			
$Rb_2Zn[Cu]Cl_4$	4250[c]	4560[c]	7330[c]	8260[c]			
Cs_2CuCl_4	4840[c]	5850[c]	8200[c]	9130[c]			

[a] Assignments are in the C_{2v} point group in the "d-d" region and in the D_{2d} point group for the charge-transfer region. [b] Polarized crystal measurements made at ~8 K. [c] Measurements made by reflectance at 295 K.

Table V. Principal Molecular g Values and Their Orientation in the Molecular Coordinate System[a]

	$(enH_2)_2Zn[Cu]Cl_6$	$Cs_2Zn[Cu]Cl_4$	$Rb_2Zn[Cu]Cl_4$
g_x	2.0077 (5)	2.078 (4)	2.078 (5)
g_y	2.2103 (6)	2.080 (4)	2.109 (5)
g_z	2.4356 (6)	2.437 (3)	2.413 (5)
eigenvectors	0.999, −0.050, 0.000	−0.986, 0.007, 0.167	−0.999, 0.000, −0.043
	−0.050, −0.999, 0.000	0.007, 1.000, 0.001	0.000, 1.000, 0.000
	0.000, 0.000, 1.000	0.167, 0.001, 0.986	−0.043, 0.000, 0.999

[a] See text for definition of the molecular coordinate systems.

work was not obtained, the room-temperature reflectance spectrum of the compound revealed bands at 5360 and 4420 cm^{-1} that are assigned to the transitions $^2A_1(d_{x^2-y^2}) \rightarrow {}^2B_1(d_{xz})$ and $^2A_1(d_{x^2-y^2}) \rightarrow {}^2B_2(d_{yz})$, respectively. The reflectance spectrum of $Rb_2Zn[Cu]Cl_4$ was also recorded, and the observed transition energies and their assignments are listed in Table IV together with those of pure Cs_2CuCl_4 for comparison.

Charge-Transfer Region (22 000–30 000 cm^{-1}). The crystal spectra of $(enH_2)_2Zn[Cu]Cl_6$ and $Cs_2Zn[Cu]Cl_4$ in this region are quite similar (Figure 4), consisting of weak bands centered at ~23 400 and 29 000 cm^{-1} and a more intense doublet centered at ~25 000 cm^{-1}. Simple molecular orbital calculations on a model $CuCl_4^{2-}$ complex of D_{2d} symmetry suggest[13,14] that the lowest energy charge-transfer states are due to electron transfers involving chloride π orbitals of A_2, E, and B_2 symmetries, in order of increasing transition energy. The transition to the state of E symmetry is allowed in x,y polarization, while those to the other two states are formally forbidden. The observed polarization properties of the bands and their relative intensities are thus consistent with the assignments shown in Table IV, the E state being split by the lowering of the symmetry from D_{2d} to C_{2v}.[30] The fact that the $^2E \leftarrow {}^2B_2$ charge-transfer transition is ~12 times as intense as the $^2A_1(d_{z^2}) \leftarrow {}^2B_2(d_{xy})$ "d–d" transition is in good agreement with theoretical calculations.[7]

EPR Parameters of the Complexes. The molecular **g** tensors were derived from the measured crystal g values by a method given in detail elsewhere.[31] This consists in essence of describing the g value obtained from each measured EPR signal by an equation of the form

$$g^2 = x^2g_{xx}^2 + y^2g_{yy}^2 + z^2g_{zz}^2 + 2xyg_{xy}^2 + 2xzg_{xz}^2 + 2yzg_{yz}^2 \quad (1)$$

where x, y, and z are the direction cosines between the magnetic field vector and the molecular axes, defined as in Figure 5. The "best fit" **g**-tensor elements g_{xx} etc. are determined by a least-squares procedure, and the principal molecular g values are obtained by diagonalization of this tensor. In each of the present complexes studied, two different molecular orientations occur for a rotation in a plane orthogonal to a crystal axis except when the magnetic field lies along a crystal axis, when all molecules are equivalent. When a single EPR signal is observed, as was the case for two of the three rotations (Figure 3), this means that the same g value (within experimental error) is associated with both sets of molecular projections. When two EPR signals are seen, as was the case in the third rotation for each compound, a choice must be made between which g value is associated with which set of molecular projections. The calculations were performed for both choices, but only one of these produced chemically reasonable g values and an orientation of the **g** tensor that was related in any meaningful way to the geometry of the host complex. The principal g values for each complex are shown in Table V, together with the corresponding eigenvectors, these representing the direction cosines between the principal g axes and the molecular axes. The small values of the off-diagonal elements of the eigenvector matrices show that the principal g axes and molecular axes are almost exactly coincident (the largest deviation is 2.5° for $(enH_2)_2Zn[Cu]Cl_6$ and $Rb_2Zn[Cu]Cl_4$ and 9.5° for $Cs_2Zn[Cu]Cl_4$).

It may be noted that the EPR parameters of $(enH_2)_2Zn[Cu]Cl_6$ could be determined considerably more accurately than those of $Cs_2Zn[Cu]Cl_4$ and $Rb_2Zn[Cu]Cl_4$, because of the better resolution of the spectra of the former compound. Also, the reason why each compound exhibits one signal for two crystal rotations, but two for the third, now becomes apparent. For the two former rotations the projections of the magnetic field on the molecular coordinates of the two different molecules are approximately equal for all crystal orientations, while for the latter rotations this is not the case. In fact, when the magnetic field lies midway between the b and c axes of $(enH_2)_2Zn[Cu]Cl_6$, it lies approximately parallel to the z axis of one $CuCl_4^{2-}$ ion and the y axis of the second independent $CuCl_4^{2-}$ ion, so that the spectra of these two species are fully resolved (Figure 2). A similar situation occurs for $Cs_2Zn[Cu]Cl_4$ and $Rb_2Zn[Cu]Cl_4$, except that here the axes involved are z and x.

As mentioned above, the spectra of all three compounds were broad and ill-defined at 295 K but sharpened considerably on cooling to 120 K, at which temperature the spectra used to derive the molecular **g** tensors were recorded. It seems likely that the broadening at room temperature is caused by rapid relaxation effects, related to the comparatively low energy of the first excited electronic states of the complexes (~4500 cm^{-1}). It is improbable that the broadening is due to dynamic

(30) It has recently been suggested that the band at ~29 000 cm^{-1} in distorted-tetrahedral $CuCl_4^{2-}$ complexes is due to the transition $^2E(T_2) \leftarrow {}^2B_2$, rather than $^2B_2(T_2) \leftarrow {}^2B_2$ as suggested above. Solomon, E., private communication.

(31) Hitchman, M. A.; Belford, R. L. "Electron Spin Resonance of Metal Complexes"; Yen, Tek Fu, Ed.; Plenum Press: New York, 1969; p 97.

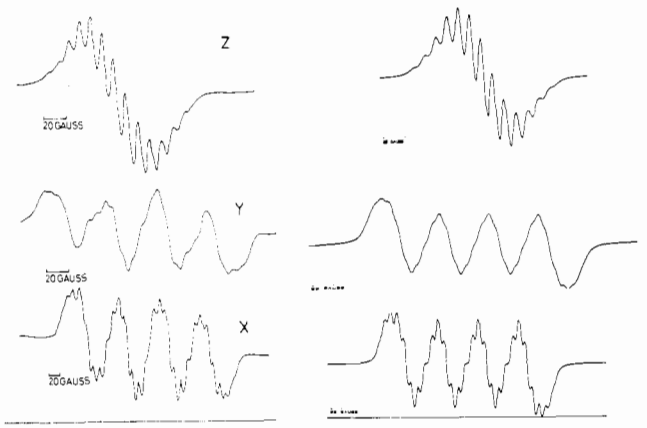

Figure 6. Observed (left) and computer-simulated (right) EPR spectra of $(enH_2)_2Zn[Cu]Cl_6$ with the magnetic field along the x, y, and z molecular axes.

vibrational effects, as no significant shifts in the positions of the peaks are observed.

EPR Parameters of $(enH_2)_2Zn[Cu]Cl_6$. Superhyperfine Parameters. For this complex, the single broad line observed at room temperature when the magnetic field was aligned with the molecular x or y axis was resolved into four components when the temperature was lowered to 103 K. This effect is assigned to hyperfine coupling with the copper nuclear spin ($I = {}^3/_2$). On cooling to 77 K, each of these lines was further split into seven, equally spaced components (for the complexes $Cs_2Zn[Cu]Cl_4$ and $Rb_2Zn[Cu]Cl_4$ no structure was resolved, even on cooling to 77 K). Furthermore, at 77 K, the single line observed when the magnetic field was parallel to the z axis was resolved into 13, equally spaced lines. The spectra observed for these three orientations of $(enH_2)_2Zn[Cu]Cl_6$ at 77 K are shown in Figure 6. The seven-line pattern, which is resolved clearly when the magnetic field is parallel to the x molecular axis but only poorly when it is parallel to the y axis, is assigned to a superhyperfine coupling with two chloride ligands (nuclear spin $I = {}^3/_2$).

Superhyperfine coupling involving chlorine nuclei has been reported for copper doped into the planar complex K_2PdCl_4,[32] the superhyperfine tensor elements for each of the four equivalent chloride ligands being found to have the magnitudes $|A_{z'}| = 23.3 \times 10^{-4}$ cm^{-1} and $|A_{x'}| = |A_{y'}| = 5.3 \times 10^{-4}$ cm^{-1}, where z' was defined to lie along the Cu–Cl bond direction. In $(enH_2)_2Zn[Cu]Cl_6$ the situation is more complicated than is the case for $K_2Pd[Cu]Cl_4$. This is because each $CuCl_4^{2-}$ unit contains two different types of chlorine atom as a result of the marked difference between the $\angle ClCuCl$ angles (these being estimated to be $\sim$135 and $\sim$113°; see following section). In the following discussion the ligands subtending the angle α are labeled Cl(1), while those subtending β are labeled Cl(2). The slight difference in bond distance between the two atoms of type 2 (0.04 Å in the zinc host) is assumed to have a negligible effect on the superhyperfine parameters. Moreover, whereas in the planar $CuCl_4^{2-}$ ions present in $K_2Pd[Cu]Cl_4$ the metal–ligand bond directions coincide with the molecular x and y axes and the lobes of the metal $d_{x^2-y^2}$ orbital, this is no longer the case for the distorted $CuCl_4^{2-}$ ions present in $(enH_2)_2Zn[Cu]Cl_6$. This means that while in the former complex the z' axes of the superhyperfine tensor of each chlorine is required by symmetry to lie along the metal–ligand bond direction and it is likely that the magnitude of the two other superhyperfine tensor elements are approximately equal, in $(enH_2)_2Zn[Cu]Cl_6$ the principal z' direction of the superhyperfine tensor could well deviate from the Cu–Cl bond direction,[33] and $A_{x'}$ could differ substantially from $A_{y'}$.

(32) Chow, C.; Chang, K.; Willett, R. D. *J. Chem. Phys.* **1973**, *59*, 2629.

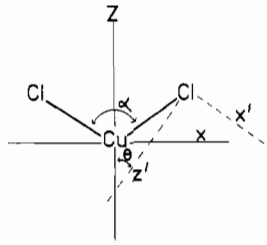

Figure 7. Schematic diagram showing the principal x' and z' superhyperfine axes of type 1 chlorine atoms in $(enH_2)_2Zn[Cu]Cl_6$.

Table VI. Magnitudes of the Hyperfine and Superhyperfine Splitting Parameters ($cm^{-1} \times 10^4$) When the Magnetic Field Is Parallel to the Molecular Axes in $(enH_2)_2Zn[Cu]Cl_6$

axis	Cu	Cl(1)[a]	Cl(2)[b]
x	71.3	10.7	2.9
y	43.2	4.2	7.4
z	2.3	11.2	11.2

[a] Chlorine atoms subtending larger angle at the metal. [b] Chlorine atoms subtending smaller angle at the metal.

The principal superhyperfine coordinate system of the Cl(1) ligands is illustrated in Figure 7. Note that the y' axes of type 1 ligands are parallel to the y molecular axis, while the y' axis of type 2 ligands are parallel to the x molecular axis. The z',x' axes of type 1 ligands thus lie in the zx molecular plane, while the z',x' axes of type 2 ligands lie in the zy molecular plane. The seven-line pattern observed when the magnetic field is parallel to the x molecular axis is assigned to coupling with the two Cl(1) nuclei, the interaction with the two type 2 ligand nuclei, for which the field is coincident with the y' axes, being assumed to be so small that it merely broadens the signals. Similarly, when the magnetic field is parallel to the y molecular axis, the dominant splitting is due to the interaction with the two type 2 ligand nuclei, the effect of the type 1 ligand nuclei serving merely to broaden the signals. The 13-line pattern observed when the magnetic field lies along the z molecular axis is assumed to be due to coupling with all four chlorine nuclei, with the inequivalence of the two pairs of ligands and the metal hyperfine splitting, which is not resolved in this orientation, serving to broaden the lines. When the observed patterns were assigned in this manner, spectral simulations were carried out in which the magnitudes of the superhyperfine splitting parameters and, for the z molecular spectrum, the metal hyperfine splitting, were varied until optimum agreement with the experimental spectra was obtained. The simulated spectra are shown in Figure 6, while the "best fit" superhyperfine values measured along the directions of the molecular x, y, and z axes are given in Table VI. The fit was quite sensitive to the parameters used, the estimated error limits being $\pm 0.3 \times 10^{-4}$ cm^{-1}. The superhyperfine parameters (in cm^{-1}) were deduced from the observed spectral splittings by using the relationship

$$A\ (\text{cm}^{-1}) = 4.6686 \times 10^{-5} gA\ (\text{G})$$

Given the above magnitudes of the superhyperfine parameters measured with the magnetic field along each molecular axis direction, it is clearly of interest to attempt to derive the principal magnitudes and directions of the superhyperfine tensor of each type of chlorine. The only principal superhyperfine axis that is defined by symmetry is $A_{y'}$, this being parallel to the y molecular axis for Cl(1) and the x molecular

(33) We are grateful to Professor R. L. Belford, University of Illinois, Urbana—Champagne, and Professor B. R. McGarvey, University of Windsor, for pointing out the possibility that the metal–chlorine bond direction might well not coincide with a principal superhyperfine axis.

Table VII. Range of Possible Principal Superhyperfine Parameters ($cm^{-1} \times 10^4$) for the Chlorine Atoms in $(enH_2)_2Zn[Cu]Cl_6$

Cl(1)[a]				Cl(2)[a]			
$\|A_{z'}\|$	$\|A_{x'}\|$	$\|A_{y'}\|$[b]	θ[c]	$\|A_{z'}\|$	$\|A_{x'}\|$	$\|A_{y'}\|$	θ[c]
11.5	10.4	4.2	31.8	11.5	6.9	2.9	16.5
12.0	9.8		38.4	12.0	6.0		24.5
12.5	9.2		40.7	12.5	4.9		28.9
13.0	8.4		41.8	13.0	3.4		31.7
13.5	7.6		42.5				
14.0	6.6		42.9				
14.5	5.5		43.3				
15.0	3.9		43.5				

[a] The maximum possible value of $A_{z'}$ or $A_{x'}$ is 15.5×10^{-4} cm^{-1} for Cl(1) and 13.4×10^{-4} cm^{-1} for Cl(2). [b] The magnitude of $A_{y'}$ is independent of θ. [c] Angle (deg) between z' and the molecular z axis; see Figure 7.

axis for Cl(2) (Figure 7). The magnitudes of this parameter are therefore $A_{y'} = (4.2 \pm 0.3) \times 10^{-4}$ and $(2.9 \pm 0.3) \times 10^{-4}$ cm^{-1} for Cl(1) and Cl(2), respectively (Table VI). These may be compared with the value of $A_{x'} = A_{y'} = 5.3 \times 10^{-4}$ cm^{-1} reported[32] for the superhyperfine tensor of the chloride ions in the planar complex present in $K_2Pd[Cu]Cl_4$. Since on going from the planar to the distorted-tetrahedral geometry the overlap between the chlorine orbitals and the copper(II) $d_{x^2-y^2}$ orbital containing the unpaired electron decreases, it is expected that the magnitude of $A_{y'}$ should also decrease, as is observed experimentally. Moreover, the decrease should be more pronounced for the chloride ions subtending the smaller angle at the metal, Cl(2), again in agreement with experiment.

Sufficient experimental data are not available to determine the principal values and directions of $A_{z'}$ and $A_{x'}$ uniquely. However, it is interesting to look at the possible ranges that these parameters may take. If the angle between the z' superhyperfine axis and the z molecular axis is θ, as illustrated in Figure 7 for the Cl(1) atoms, then the measured superhyperfine parameters are related to the principal values by

$$A_z^2 = A_{z'}^2 \cos^2 \theta + A_{x'}^2 \sin^2 \theta \quad (2a)$$

$$A_x^2 = A_{z'}^2 \sin^2 \theta + A_{x'}^2 \cos^2 \theta \quad (2b)$$

for Cl(1) and

$$A_z^2 = A_{z'}^2 \cos^2 \theta + A_{x'}^2 \sin^2 \theta \quad (2c)$$

$$A_y^2 = A_{z'}^2 \sin^2 \theta + A_{x'}^2 \cos^2 \theta \quad (2d)$$

for Cl(2).

Substitution of the appropriate values for A_x, A_y, and A_z (Table VI) produces the possible ranges of values for the principal superhyperfine parameters and the angle θ defining their directions listed in Table VII. These may be compared with the values $A_{z'} = 23.3 \times 10^{-4}$ cm^{-1} and $A_{y'} = 5.3 \times 10^{-4}$ cm^{-1} reported for planar $K_2Pd[Cu]Cl_4$. The comparatively small values of $A_{x'}$ and $A_{y'}$ for the planar complex are due to the fact that the isotropic interaction from the unpaired electron density in the chlorine 3s orbital acts in an opposite sense to the dipolar contribution from the chlorine $p_{z'}$ unpaired spin density. The much larger value of $A_{z'}$ is due to the fact that the dipolar contribution from the chlorine $p_{z'}$ orbital that overlaps with the copper $d_{x^2-y^2}$ orbital then acts in the same sense as the isotropic component. On going from the planar to the distorted-tetrahedral geometry, it is expected that the overlap between the $d_{x^2-y^2}$ orbital and the chlorine $p_{z'}$ orbital should decrease, while the overlap with the chlorine $p_{x'}$ orbital become nonzero. Thus, the magnitude of $A_{z'}$ is expected to decrease, while that of $A_{x'}$ should increase. Inspection of the possible values in Table VII shows that $A_{z'}$ for the chlorides in the distorted-tetrahedral $CuCl_4^{2-}$ ion in $(enH_2)_2Zn[Cu]Cl_6$ must indeed be significantly smaller than that in planar $CuCl_4^{2-}$. Moreover, as expected, the decrease is likely to be greater for the chloride ions subtending the smaller angle at the metal. It is noteworthy that a self-consistent set of parameters for the two types of chloride ion can only be obtained for a quite limited range of angles θ, namely $\theta \approx 42°$ for Cl(1) and $\theta \approx 25°$ for Cl(2), corresponding to principal superhyperfine values $A_{z'} \approx 14 \times 10^{-4}$ cm^{-1}, $A_{x'} \approx 7 \times 10^{-4}$ cm^{-1} and $A_{z'} \approx 12 \times 10^{-4}$ cm^{-1}, $A_{x'} \approx 6 \times 10^{-4}$ cm^{-1}, respectively. These angles may be compared with those subtended by the metal–chloride bond vectors, which are estimated as ~68° for Cl(1) and ~57° for Cl(2) (see following section). It thus appears that the principal superhyperfine z' axes deviate substantially from the Cu–Cl directions, as indicated schematically in Figure 7. In fact, it seems likely that the superhyperfine axes of both kinds of chloride cut the molecular x or y axis at a distance of ~1.3 Å from the metal ion. Possibly this is influenced by the fact that the bulk of the unpaired electron density is located in the $d_{x^2-y^2}$ orbital and will hence be delocalized along these two directions.

Superhyperfine coupling involving chlorine nuclei has been reported in two other copper-doped pseudotetrahedral complexes, dichlorobis(triphenylphosphine oxide)zinc(II), $(Ph_3PO)_2Zn[Cu]Cl_2$,[34] and dichloro(1,10-phenanthroline)-zinc(II), (*o*-phen)$Zn[Cu]Cl_2$.[35] In the former complex, maximum and minimum values of 17×10^{-4} and $\sim 7 \times 10^{-4}$ cm^{-1} for the coupling constant were reported,[34] but the orientation of the superhyperfine tensor was not investigated quantitatively. In the latter compound, the orientation of the superhyperfine tensor was again apparently not studied in detail but was discussed[35] in terms of the axially symmetric values $A_{\parallel}' = (19.3 \pm 1.5) \times 10^{-4}$ cm^{-1} and $A_{\perp}' = (4.9 \pm 1.5) \times 10^{-4}$ cm^{-1}. These are in broad agreement with the present results, but in view of the apparent noncoincidence of the principal superhyperfine axes and the Cu–Cl bond vectors and the rhombic nature of the superhyperfine parameters in $(enH_2)_2Zn[Cu]Cl_6$, it would clearly be of some interest to study other pseudotetrahedral halide complexes to determine more accurately the way in which the superhyperfine tensor varies as a function of the geometry of the complex.

Unpaired Electron Density Distribution among the Chlorine Orbitals from the Superhyperfine Parameters. The principal superhyperfine values may be broken down into an isotropic component A_s', due to the contribution from the occupancy of the chlorine 3s orbital, and dipolar components due to the occupancy of the chlorine 3p orbitals. In the present situation both the chlorine $3p_{z'}$ and $3p_{x'}$ orbitals may overlap with the metal $d_{x^2-y^2}$ orbital and will give dipolar contributions $A_{pz'}$ and $A_{px'}$. In addition, a small dipolar contribution, $A_{D'}$, from the unpaired electron density on the metal will occur. This latter may be estimated as $\sim 0.14 \times 10^{-4}$ cm^{-1} and can be assumed to maximize along the z' direction.[35] Assuming that each interaction is due directly to the unpaired electron density in the orbital in question, all of these components are positive. The relationships between the above parameters have been given elsewhere[35] for an axially symmetric superhyperfine tensor, and the expressions are readily extended to the rhombic situation observed for $(enH_2)_2Zn[Cu]Cl_6$, yielding eq 3a–c.

$$A_{x'} = A_{s'} + 2A_{px'} - A_{pz'} - A_{D'} \quad (3a)$$

$$A_{y'} = A_{s'} - A_{px'} - A_{pz'} - A_{D'} \quad (3b)$$

$$A_{z'} = A_{s'} + 2A_{pz'} - A_{px'} + 2A_{D'} \quad (3c)$$

Substitution of the values $A_{x'} \simeq 7$, $A_{y'} \simeq 4$, $A_{z'} \simeq 14$ and $A_{x'}$

(34) Bencini, A.; Gatteschi, D.; Zanchini, C. *J. Am. Chem. Soc.* **1980**, *102*, 5234.
(35) Kokoszka, G. F.; Reimann, C. W.; Allen, H. C., Jr. *J. Phys. Chem.* **1967**, *71*, 121.

Table VIII. Approximate Fractional Unpaired Electron Density in the Chlorine 3s and 3p Orbitals in $(enH_2)_2Zn[Cu]Cl_6$ and Related Compounds[a]

compd	% fractional occupancy 3s	$3p_{x'}$	$3p_{z'}$	total 3p
$(enH_2)_2Zn[Cu]Cl_6$ Cl(1)	0.6	1.4	4.4	5.8
Cl(2)	0.5	1.4	4.0	5.4
(1,10-phen)Zn[Cu]Cl_2[b]	0.7			6.7
$K_2Pd[Cu]Cl_4$[c]	0.8			6.0

[a] Estimated neglecting spin polarization effects; see text for the method of calculation. [b] Data from ref 35. [c] Data from ref 32.

$\simeq 6$, $A_{y'} \simeq 3$, and $A_{z'} \simeq 12$ for the chloride ions of types 1 and 2, respectively, yields the values $A_{s'} = 8.3$, $A_{pz'} \simeq 3.2$, and $A_{px'} \simeq 1.0$ and $A_{s'} \simeq 7.0$, $A_{pz'} \simeq 2.9$, and $A_{px'} \simeq 1.0$, for chlorines of types 1 and 2, all in units of 10^{-4} cm^{-1}. While the signs of the superhyperfine splittings $A_{x'}$, $A_{y'}$, and $A_{z'}$ could not be determined experimentally, negative values are rendered impossible by the restriction that $A_{s'}$, $A_{px'}$, and $A_{pz'}$ must be positive. The isotropic and dipolar terms may be related to the unpaired electron density in the s and p orbitals f_s and f_p via[35]

$$A_{s'} = \frac{16\pi\gamma\beta\beta_N}{3} f_{s'} |S(0)|^2 \quad (4a)$$

$$A_{p'} = \frac{4\gamma\beta\beta_N}{5} f_{p'} \langle r^{-3}{}_p \rangle \quad (4b)$$

The substitution of the appropriate values[35] of $|S(0)|^2$ and $\langle r^{-3}{}_p \rangle$ in these equations leads to the estimated orbital occupancies shown in Table VIII, together with those calculated for the chloride ions in planar $K_2Pd[Cu]Cl_4$ and pseudotetrahedral (*o*-phen)Zn[Cu]Cl_2 for comparison. It should be noted that the limitations on the knowledge of $A_{x'}$ and $A_{z'}$ discussed above mean that the distribution of the unpaired electron between the $p_{x'}$ and $p_{z'}$ orbitals is known only imprecisely but that within the limitations of the model the total occupancy of the s and p orbitals can be estimated reasonably accurately. The values deduced for $(enH_2)_2Zn[Cu]Cl_6$ agree well with those calculated for the other two complexes and suggest a ratio of s/p orbital occupancy of ~0.1 and that the unpaired electron spends ~13% of its time in Cl(1) orbitals, ~12% in Cl(2) orbitals, and ~75% in the copper d orbitals (largely the $d_{x^2-y^2}$ orbital, but with a significant contribution from the d_{z^2} orbital; see below).

While the above interpretation probably gives an approximate guide to the unpaired electron density distribution, it has been assumed that the s-orbital contribution arises from a direct covalent interaction, with spin polarization effects being negligible. While available experimental evidence tends to support this supposition,[53] the above conclusions concerning the s and p-orbital participation in the ground-state wave functions must be viewed with caution.

Molecular *g* Values. The *g* values of $(enH_2)_2Zn[Cu]Cl_6$ are highly rhombic (Table V) and may therefore only be interpreted in terms of an effective molecular point group of, at highest, C_{2v} symmetry. In this point group the $d_{x^2-y^2}$ and d_{z^2} orbitals both transform in the A_1 representation so that the metal part of the ground-state wave function is a mixture of these orbitals: $\psi = ad_{x^2-y^2} - bd_{z^2}$, where $a^2 + b^2 = 1$. Simple first-order perturbation theory gives eq 5a–c for the *g* shifts

$$\Delta g_x = -2\lambda k_x^2 (a - 3^{1/2}b)^2 / E_{yz} \quad (5a)$$

$$\Delta g_y = -2\lambda k_y^2 (a + 3^{1/2}b)^2 / E_{xz} \quad (5b)$$

$$\Delta g_z = -8\lambda k_z^2 a^2 / E_{xy} \quad (5c)$$

from the free-electron value. Here λ is the spin–orbital coupling constant of the copper ion (-828 cm^{-1}), E is the energy of the excited state in which the unpaired electron occupies the d orbital indicated by the subscript, and $k_{x,y,z}$ are orbital reduction parameters.[36] Insufficient data are available to allow the estimation of all three orbital reduction parameters and the mixing coefficients a and b. Moreover, the crudity of this essentially ionic model does not justify drawing more than broad conclusions about the nature of the ground state. If it is assumed that $k_x^2 \approx k_y^2$ then substitution of the appropriate values of E_{xz} and E_{yz} (Table IV) and λ in eq 5a,b yields the value $k_x^2 = k_y^2 \approx 0.33$, in reasonable agreement with the value of $k_\perp^2 = 0.25$ derived for axially symmetric pseudotetrahedral $CuCl_4^{2-}$ ions.[1] Substitution of this value in eq 5a–c produces the results $b \approx 0.27$, $a \approx 0.96$, and $k_z^2 \approx 0.55$. The latter orbital reduction parameter agrees well with the value of $k_\parallel^2 \approx 0.5$, estimated for the axially symmetric pseudotetrahedral $CuCl_4^{2-}$ ions.[1] Even if it is assumed that $k_x \neq k_y$ and k_x^2 and k_y^2 are varied independently over the range 0.25–0.5, this only introduces an uncertainty in the coefficient b of ± 0.08.

The molecular *g* values thus strongly suggest that the metal part of the ground-state wave function, which for a tetragonally symmetric $CuCl_4^{2-}$ ion in the absence of spin–orbit coupling is composed purely of the $3d_{x^2-y^2}$ orbital[37] (neglecting any small admixture of the metal p orbitals), is significantly contaminated by the $3d_{z^2}$ orbital in $(enH_2)_2Zn[Cu]Cl_6$. The effect of the contamination has been discussed in detail elsewhere,[38,39] this being to create a new wave function of the form

$$\psi = KR/r^2 |cx^2 + ey^2 + fz^2\rangle$$

where K is a constant and R the radial distribution function. The constants c, e, and f are related to the coefficients a and b by the expressions $c = b + 3^{1/2}a$, $e = b - 3^{1/2}a$, and $f = -2b$ and in $(enH_2)_2Zn[Cu]Cl_6$ these take the values $c \approx 1.93$, $e \approx -1.39$, and $f \approx -0.54$. Note that for a pure $d_{x^2-y^2}$ orbital $c = e = 3^{1/2}$ and $f = 0$, while when $b = 0.5$, the ground state becomes d_{x^2}, with $c = 2$ and $e = f = -1$. The participation of the d_{z^2} orbital in the ground state thus creates a wave function in which the lobe along the x molecular axis is expanded and that along y contracted, relative to a pure $d_{x^2-y^2}$ orbital. In addition, a ground-state lobe also now occurs along the z molecular axis. For $(enH_2)_2Zn[Cu]Cl_6$ the coefficient f lies approximately midway between 0 and -1, so that the ground-state wave function is an essentially equal admixture of $d_{x^2-y^2}$ and the unconventional d function d_{x^2} (more properly written $d_{2x^2-z^2-y^2}$). The cause of the orbital mixing lies, of course, in the fact that the symmetry of the complex is no longer axial but rhombic, and since for copper(II) the ground state is in effect occupied by a positive hole, simple theory predicts that the largest ground-state lobe, that along x, should be directed toward the strongest ligand perturbation. Experimental evidence is available for many copper(II) complexes of rhombic symmetry[24,38,39] to suggest that this is indeed the case in practice, and this is also supported by the calculations on $(enH_2)_2Zn[Cu]Cl_6$ (see subsequent section).

Copper Hyperfine Parameters. It has been recognized, for some time,[34,35,40,41] that the hyperfine parameters of pseudo-

(36) Gerloch, M.; Miller, J. R. *Prog. Inorg. Chem.* **1968**, *10*, 1.
(37) Actually for a complex of D_{2d} symmetry with the axes defined in the conventional manner, the ground-state orbital is $3d_{xy}$ rather than $3d_{x^2-y^2}$. This simply reflects a rotation of 45° in the orientation of the x and y coordinates.
(38) Hitchman, M. A.; Olsen, C. D.; Belford, R. L. *J. Chem. Phys.* **1969**, *50*, 1195.
(39) Hitchman, M. A. *J. Chem. Soc. A* **1970**, 4.
(40) Bertini, I.; Canti, G.; Grassi, R.; Scozyafava, A. *Inorg. Chem.* **1980**, *19*, 2198.
(41) Fee, J. A. *Struct. Bonding (Berlin)* **1975**, *23*, 1.

Table IX. Observed and Calculated Copper Hyperfine Parameters ($cm^{-1} \times 10^4$) for $(enH_2)_2Zn[Cu]Cl_6$ and Related Compounds

compd	obsd			calcd			K^a	P,[a] $cm^{-1} \times 10^4$
	$\|A_x\|$	$\|A_y\|$	$\|A_z\|$	A_x	A_y	A_z		
$(enH_2)_2Zn[Cu]Cl_6$	71.3	43.2	2.3	67	47	2	0.10	275
$Cs_2Zn[Cu]Cl_4$[b]	48.5		25	52		−18	0.15	300
$K_2Pd[Cu]Cl_4$[c]	34.5		164	−24		−165	0.43	330

[a] Values used to obtain calculated parameters. [b] Experimental data from ref 15. [c] Experimental data from ref 32.

tetrahedral copper(II) complexes cannot be explained satisfactorily by means of the simple expressions conventionally used to interpret the parameters of planar or pseudooctahedral complexes (eq 6a–c).[42] Here, a and b are the mixing coefficients of the $d_{x^2-y^2}$ and d_{z^2} orbitals, $\Delta g_{x,y,z}$ are the g shifts from the free-electron value, and α^2 represents the fractional time the unpaired electron spends in the metal d orbitals. For a free Cu^{2+} ion the parameter $P = g_e g_N \beta\beta_N \langle r^{-3} \rangle = 0.036\ cm^{-1}$,[43] while the Fermi contact parameter $K = 0.43$.[15] Data from other related systems[16] suggests $\alpha^2 \approx 0.75$ in good agreement with the analysis of the superhyperfine coupling constants of $(enH_2)_2Zn[Cu]Cl_6$.

$$A_x = P[-K\alpha^2 + 2\alpha^2(a^2 - b^2)/7 + 4(3^{1/2})\alpha^2 ab/7 + \Delta g_x - (3a - 3^{1/2}b)\Delta g_y/14(a + 3^{1/2}b) - \Delta g_z b/7a] \quad (6a)$$

$$A_y = P[-K\alpha^2 + 2\alpha^2(a^2 - b^2)/7 - 4(3^{1/2})\alpha^2 ab/7 + \Delta g_y - (3a + (3^{1/2})b)\Delta g_x/14(a - 3^{1/2}b) + \Delta g_z b/7a] \quad (6b)$$

$$A_z = P[-K\alpha^2 - 4\alpha^2(a^2 - b^2)/7 + (3a - 3^{1/2}b)\Delta g_y/14(a + 3^{1/2}b) + (3a + 3^{1/2}b)\Delta g_x/14(a - 3^{1/2}b) + \Delta g_z] \quad (6c)$$

The fact that the failure of expressions 6a–c for pseudotetrahedral copper(II) complexes is related to the coordination geometry is well illustrated by analysis of the data for the $CuCl_4^{2-}$ ion, the hyperfine parameters of which are shown in Table IX for the ion of C_{2v} symmetry present in $(enH_2)_2Zn[Cu]Cl_6$, together with those observed for the ion of D_{2d} symmetry in $Cs_2Zn[Cu]Cl_4$ and D_{4h} symmetry in $K_2Pd[Cu]Cl_4$ for comparison. For planar $CuCl_4^{2-}$ it can be seen that it is possible to calculate values of A_z and A_{xy} in good agreement with experiment by using values of P and K quite similar to those for the free ion. For the distorted-tetrahedral ions in $Cs_2Zn[Cu]Cl_4$ and $(enH_2)_2Zn[Cu]Cl_6$, on the other hand, reasonable agreement can only be obtained by using values of P and K that are substantially reduced from the free-ion values. In particular, the effective value of K must be quite small, particularly in the case of $(enH_2)_2Zn[Cu]Cl_6$. In this latter complex, the fact that $A_z \approx 0$ provides a severe restriction on the possible value of K. Several explanations for the low effective values of P and K in pseudotetrahedral complexes have been proposed. In the original treatment of the EPR parameters of $Cs_2Zn[Cu]Cl_4$, Sharnoff suggested[15] that the metal 4p orbitals made a substantial contribution to the bonding, with this significantly affecting the metal hyperfine parameters. The way in which the EPR parameters vary as a function of the geometry of pseudotetrahedral copper(II) complexes has been discussed by Yokoi and co-workers,[16,44] who concluded that the distortion from a planar toward a tetrahedral stereochemistry is accompanied by a progressive decrease in K. It was inferred that while the metal 4p orbitals make a slight contribution to the bonding, the dominant cause of the low value of K is a 3d–4s spin-polarization effect. More recently, Bencini et al.[34] also suggested that metal 4p-orbital participation is unlikely to be significant in this kind of compound, and these authors proposed that the large spin–orbit coupling constant of chlorine, combined with the relatively high covalency of the copper–chlorine bonds, may make it invalid to use the simple formulas (6a)–(6c) to interpret the EPR parameters of chlorocuprate complexes. The situation in $(enH_2)_2Zn[Cu]Cl_6$ is complicated by the fact that the marked departure from tetragonal symmetry of the $CuCl_4^{2-}$ ion means that the metal 4s orbital may mix directly into the ground-state wave function, and this could cause a depression of the Fermi contact term. This effect is quite well established for low-spin cobalt(II) complexes.[45] Moreover, for copper-doped NH_4Br, in which the unpaired electron occupies the d_{z^2} orbital, the low value of K (0.02) has been rationalized[46] in terms of the direct participation of the metal 4s orbital in the ground-state wave functions.

Deduction of the Geometries of the Guest $CuCl_4^{2-}$ Complexes Using the Angular-Overlap Model. The angular-overlap model (AOM) provides a convenient means of parameterizing the bonding in transition-metal complexes.[47,48] Within the framework of this model, the interaction between a chloride ligand and the copper d orbitals is described in terms of just two parameters, e_σ and e_π, these representing the energy by which a d orbital is raised upon interaction with the chloride orbitals of σ and π symmetry, respectively. The total d-orbital energy matrix of a complex is obtained by summing over all ligands, using the angular-overlap matrix appropriate to the symmetry of the complex. When, as in the present case, just a single ligand is involved in the complex and it is likely that all metal–ligand bond distances are similar, the d-orbital energy matrix takes a particularly simple form in which the only variables are the metal–ligand bonding parameters and the angles subtended by the ligands at the metal. Moreover, slight differences in bond distance can be accommodated by equating differences in the parameters e_σ and e_π to the calculated differences in the square of the appropriate diatomic overlap integrals between the copper 3d and ligand orbitals. In several studies it has been found that the AOM does indeed provide a self-consistent set of bonding parameters that can satisfactorily explain the spectroscopic properties of a range of chromium(III), cobalt(II), nickel(II), and copper(II) complexes.[48]

In the present context the main purpose of the AOM calculations was to deduce the likely geometry of the $CuCl_4^{2-}$ ions in the various host lattices from the observed electronic spectral transition energies and molecular g values. The basic geometry of the $CuCl_4^{2-}$ ion in each complex (Figure 5) was defined in terms of the ∠ClCuCl angles α and β. The AOM bonding parameters producing optimum agreement with the spectral observations were calculated for Cs_2CuCl_4 as a function of these angles by using the general angular-overlap matrix given by Larsen and La Mar,[49] the g values being estimated by using

(42) McGarvey, B. R. *Transition Met. Chem. (N.Y.)* **1966**, *3*, 89.
(43) McGarvey, B. R. *J. Phys. Chem.* **1967**, *71*, 51.
(44) Yokoi, H. *Bull. Chem. Soc. Jpn.* **1974**, *47*, 3037.
(45) McGarvey, B. R. *Can. J. Chem.* **1975**, *53*, 2498. Hitchman, M. A. *Inorg. Chem.* **1977**, *16*, 1985.
(46) Narayana, P. A.; Sastry, K. L. V. N. *J. Chem. Phys.* **1972**, *57*, 3266.
(47) Schaffer, C. E. *Struct. Bonding (N.Y.)* **1973**, *14*, 69. Burdett, J. K. *Ibid.* **1967**, *31*, 67.
(48) Smith, D. W. *Struct. Bonding (N.Y.)* **1978**, *35*, 87. This reference provides a summary of the application of the AOM to the interpretation of the spectroscopic properties of metal complexes.

Table X. Angular-Overlap Bonding Parameters and Calculated and Observed Spectroscopic and Structural Properties of Some Pure Tetrachlorocuprates[a]

	Cs_2CuCl_4	$(TMBA)_2CuCl_4$	$(Nmph)_2CuCl_4$
e_σ, cm^{-1}	5950	5840	5610
e_π, cm^{-1}	1300	1320	950
α, deg	130.8 (131.2)	132.1 (132.8)	179.0 (180.0)
β, deg	125.1 (127.1)	130.4 (132.1)	170.0 (180.0)
E_{yz}, cm^{-1}	4930 (4800)	6000 (5920)	14 430 (14 530)
E_{xz}, cm^{-1}	5690 (5590)	5910 (5920)	14 040 (13 840)
E_{xy}, cm^{-1}	8130 (8000)	*b*	12 560 (12 500)
E_{z^2}, cm^{-1}	8800 (9050)	8730 (8850)	*c*
g_x	2.075 (2.083)	2.071 (2.071)	2.038 (2.040)
g_y	2.085 (2.105)	2.084 (2.083)	2.042 (2.040)
g_z	2.401 (2.384)	2.387 (2.391)	2.220 (2.221)
$k_\parallel^2$	0.490	0.470	0.413
$k_\perp^2$	0.250	0.270	0.326
a	0.999	0.999	0.999
b	0.0392	0.0262	0.0200

[a] Experimental values are given in parentheses. [b] Electronic transition not observed experimentally. [c] Not included in calculation as orbital energy is affected by configuration interaction with the metal 4s orbital; see ref 11.

the expressions in eq 5a–c. The results are given in Table X, from which it may be seen that the experimental spectroscopic values are reproduced satisfactorily and that the angles α and β are within ~2° of the values obtained from an X-ray structural analysis of the complex. The ratio $e_\pi:e_\sigma$ of ~0.2 is also in good agreement with the predictions of the AOM,[10,48] which equates this to the ratio of the square of the diatomic overlap integrals between the chlorine σ and π orbitals and the copper d orbitals. It should be noted that the d orbitals are eigenfunctions of the ligand field with the exception of $d_{x^2-y^2}$ and d_{z^2}, the mixing of which in the highest energy d orbital is described by the coefficient *a* and *b*. In order to investigate the ability of the model to satisfactorily predict the stereochemistry of $CuCl_4^{2-}$ from spectral data, the geometry of two complexes of known structure containing this ion, $(TMBA)_2CuCl_4$ and $(Nmph)_2CuCl_4$, where TMBA = $[C_6H_5CH_2N(CH_3)_3]^+$ and Nmph = $[C_6H_5C_2H_4NCH_3H_2]^+$, were calculated. The parameter e_σ was fixed at the value estimated for Cs_2CuCl_4, with a slight correction for differences in the Cu–Cl bond lengths. The bonding parameter e_π, orbital reduction parameters $k_\parallel^2$ and $k_\perp^2$, and angles α and β were then varied until optimum agreement between the calculated and observed energies and *g* values was obtained. The results are presented in Table X, and for the distorted-tetrahedral ion in $(TMBA)_2CuCl_4$ the agreement between the calculated angles α and β and those deduced from the X-ray analysis is excellent. Moreover, the parameters e_π, $k_\parallel^2$, and $k_\perp^2$ are all very similar to those estimated for Cs_2CuCl_4. In the case of $(Nmph)_2CuCl_4$, which contains planar $CuCl_4^{2-}$ ions, the calculations predict a near-planar geometry (the d-orbital energies are rather insensitive to α and β as these approach 180°). However, as might be expected from the drastically different geometry, the parameters e_π, $k_\parallel^2$, and $k_\perp^2$ now differ somewhat from those calculated for Cs_2CuCl_4.

Having established the feasibility of the model to deduce the $CuCl_4^{2-}$ geometry from spectral data, the method was applied to the guest ions in the various zinc host lattices. It was not feasible to allow all the bonding parameters and the geometry of the complexes to act as independent variables in the fitting of the spectral measurements. The values of e_σ, $k_\parallel^2$, and $k_\perp^2$ were therefore set equal to those estimated for Cs_2CuCl_4 (slight corrections in the e_σ parameters of individual chloride ions were introduced, to take into account the different bond distances observed for the host $ZnCl_4^{2-}$ ions (Table I)). The angles α and β, and the bonding parameter e_π, were varied until optimum agreement between the calculated and observed spectral parameters was obtained. The results are shown in Table XI. In order to test the sensitivity of α and β to the choice of e_σ, $k_\parallel^2$, and $k_\perp^2$, these were varied within reasonable limits (10%). The angles were quite insensitive to the orbital reduction parameters. Varying e_σ caused a slight change in the average value of the angles but had little effect on their difference. All in all it is estimated that the uncertainty in the average values of α and β is ~3° for $CsZn[Cu]Cl_4$ and $RbZn[Cu]Cl_4$ and ~6° for $(enH_2)_2Zn[Cu]Cl_6$, with the uncertainty in the difference between the angles being about half these values. In the case of $(enH_2)_2Zn[Cu]Cl_6$ the *g* values and electronic excitation energies were also calculated by using the CAMMAG ligand field program developed by Gerloch and co-workers.[50,52] This explicitly includes both spin–orbit coupling and the metal–ligand interaction in the d-orbital energy matrix. Optimum agreement with experiment was obtained with ∠ClCuCl angles and bonding parameters very similar to those of the present calculations.

Table XI. Optimal Structural and Spectroscopic Parameters Estimated for Doped $CuCl_4^{2-}$ Ions[a]

	$(enH_2)_2Zn[Cu]Cl_6$	$Cs_2Zn[Cu]Cl_4$	$Rb_2Zn[Cu]Cl_4$
e_σ[b]	5950	5950	5950
e_π	1440	1470	1420
α,[c] deg	135.5 (125.4)	126.7 (115.3)	127.1 (114.3)
β,[c] deg	113.0 (107.5)	123.2 (109.0)	122.6 (107.3)
E_{yz}	4150 (4420)	4241 (4250)	4187 (4250)
E_{xz}	5200 (5360)	4586 (4560)	4613 (4560)
E_{xy}	7650 (7700)	7370 (7330)	7483 (7330)
E_{z^2}	8690 (8950)	8248 (8260)	8302 (8260)
g_x	2.0280 (2.0077)	2.090 (2.078)	2.088 (2.078)
g_y	2.1890 (2.2013)	2.102 (2.080)	2.105 (2.109)
g_z	2.4028 (2.4356)	2.442 (2.437)	2.435 (2.413)
$k_\parallel^2$[b]	0.49	0.49	0.49
$k_\perp^2$[b]	0.25	0.25	0.25
a	0.970	0.999	0.999
b	0.231	0.0307	0.0398

[a] Experimental values are given in parentheses. [b] Value of this parameter fixed in the fitting procedure. [c] Value in parentheses is the angle observed in the zinc host lattice.

The angles ∠ClZnCl of the host lattices are also shown in Table XI. It may be seen that the value of both α and β is significantly greater (10 ± 4°) in the guest copper complex than the zinc host. This expansion is presumably due to the operation of the Jahn–Teller effect for the former metal, i.e. to the asymmetry of the d-electron density of the Cu^{2+} ion. The average values of α and β are essentially constant at 125° for the three copper complexes. This is marginally less than the value of ~130° observed for pure Cs_2CuCl_4 and $(TMBA)_2CuCl_4$, agreeing well with the average value θ = 125 ± 5° predicted by several calculations[8,51] of the equilibrium nuclear geometry of a free $CuCl_4^{2-}$ ion. In each case the difference between α and β mirrors that observed crystallographically in the guest $ZnCl_4^{2-}$ ion, both in the sense and

(49) Larsen, E.; La Mar, G. *J. Chem. Educ.* **1974**, *51*, 633.

(50) Gerloch, M.; McMeeking, R. F. *J. Chem. Soc., Dalton Trans.* **1975**, 2443.

(51) Felsenfeld, G. *Proc. R. Soc. London, Ser. A* **1956**, *236*, 506. Lohr, L. L.; Lipscomb, W. N. *Inorg. Chem.* **1963**, *2*, 911. Burdett, J. K. *J. Chem. Soc., Faraday Trans. 2* **1974**, *70*, 1599. Elian, M.; Hoffmann, R. *Inorg. Chem.* **1975**, *14*, 1058.

(52) Cruse, D. A.; Davies, J. E.; Gerloch, M.; Harding, J. H.; Mackey, D. J.; McMeeking, R. F. "CAMMAG, A Fortran Computing Package"; University Chemical Laboratory: Cambridge, England.

(53) For a discussion of the interpretation of superhyperfine parameters see: Abragam, A.; Bleaney, B. "Electron Paramagnetic Resonance of Transition Ions"; Clarendon Press: Oxford, 1970; Chapter 20.

approximate magnitude of the distortion. These departures from axial symmetry are presumably due to lattice perturbations and suggest a broadly similar resistance to angular deformation for the two MCl_4^{2-} ions. The magnitude of the distortion ($\alpha - \beta \approx 20°$) in $(enH_2)_2ZnCl_6$ and its guest copper complex is quite striking. It is this that causes the marked rhombic component to the ligand field, thus producing the unusual ground state in $(enH_2)_2ZnCuCl_6$. The mixing coefficient of the d_{z^2} orbital in the angular-overlap calculations $b = 0.231$ is in good agreement with the value $b \approx 0.27$ from the simple analysis of the molecular g values (see previous section).

General Conclusions. The EPR and optical spectra of copper-doped $(enH_2)_2ZnCl_6$, Cs_2ZnCl_4, and Rb_2ZnCl_4 suggest that the guest $CuCl_4^{2-}$ ions in each case adopt a distorted-tetrahedral geometry. At 77 K the EPR spectrum of $(enH_2)_2Zn[Cu]Cl_6$ shows both hyperfine and superhyperfine structure. The chlorine superhyperfine tensors show a marked rhombic character, and the principal axes of these probably deviate significantly from the copper–chlorine bond directions. It is likely that this deviation is caused by the noncoincidence of the bond axes and the $d_{x^2-y^2}$ orbital lobe directions. It would therefore be of interest to study the anisotropy of the superhyperfine structure in other pseudotetrahedral chlorocuprate complexes. Angular-overlap calculations have been used to deduce the likely geometry of the $CuCl_4^{2-}$ guest ions, and in each case the distortions from a regular tetrahedral ligand arrangement can be interpreted in terms of an overall flattening caused by the asymmetry of the Cu^{2+} d-electron density, plus a rhombic component due to lattice perturbations. In $(enH_2)_2Zn[Cu]Cl_6$ the rhombic distortion is substantial, involving a difference of ~20° between the two ∠ClCuCl angles containing the molecular symmetry axis. As a consequence of this, the ground-state wave function of the complex consists of a mixture of the $d_{x^2-y^2}$ and d_{z^2} orbitals. Calculations of the kind described may prove of value in deducing the probable ligand coordination geometry of copper(II) ions in protein molecules.

Acknowledgment. The authors are indebted to the Central Science Laboratory of the University of Tasmania for providing facilities for the measurement of the EPR and low-temperature optical spectra and to J. Bignall for technical assistance. Financial assistance of the Australian Research Grants Commission (to M.A.H.) and the University of Tasmania (to R.J.D.) is gratefully acknowledged. The Humboldt Foundation and Professor D. Reinen of the Fachbereich Chemie of the University of Marburg are thanked by M.A.H. for providing financial assistance and laboratory facilities during the initial stages of the work.

Registry No. $(enH_2)_2ZnCl_6$, 70281-84-4; Cs_2ZnCl_4, 13820-35-4; Rb_2ZnCl_4, 33724-11-7; $CuCl_4^{2-}$, 15489-36-8; Cu, 7440-50-8.

Supplementary Material Available: A listing of the g^2 values measured for rotations of the magnetic field for different crystal planes of the compounds (3 pages). Ordering information is given on any current masthead page.

Contribution from the Departments of Chemistry, University of Denver, Denver, Colorado 80208, and University of Colorado at Denver, Denver, Colorado 80202

Metal–Nitroxyl Interactions. 36. Single-Crystal EPR Spectra of Two Copper Porphyrins Spin Labeled with Five-Membered Nitroxyl Rings

REDDY DAMODER, KUNDALIKA M. MORE, GARETH R. EATON,* and SANDRA S. EATON

Received August 16, 1983

Single-crystal EPR spectra have been obtained for two copper porphyrins spin labeled with five-membered nitroxyl rings. Multiple conformations were observed for each of the complexes doped into zinc tetraphenylporphyrin. The dependence of the electron–electron spin–spin splittings on the orientation of the crystal in the magnetic field was analyzed to obtain the isotropic exchange and anisotropic dipolar contributions to the interaction. The interspin distance, r, ranged from 9.3 to 13.5 Å. Values of the exchange coupling constant, J, ranged from -42×10^{-4} to $+35 \times 10^{-4}$ cm^{-1}. The range of values of J was greater than was previously observed for analogous complexes containing six-membered nitroxyl rings. The greater dependence of the value of J on the molecular conformation for the five-membered nitroxyl rings than for the six-membered nitroxyl rings may explain the previously observed large solvent and temperature dependence of the values of J for complexes containing five-membered nitroxyl rings.

Introduction

EPR studies of biological systems have demonstrated the importance of spin–spin interaction.[1] For some applications of the EPR interaction information it is desirable to separate the isotropic exchange and anisotropic dipolar contributions. The dipolar term is a measure of the distance between the two interacting spins. The exchange coupling constant is dependent on the bonding pathway between the two centers on which the electrons are localized. We have recently shown that the two contributions can be separated by the analysis of frozen-solution[2] and single-crystal EPR spectra.[3-5] Since the value of the exchange coupling constant J can be measured in fluid solution, it is important to determine whether that value of J can be used to estimate values in frozen solution or single crystals. The values of J observed for I–V in fluid solution

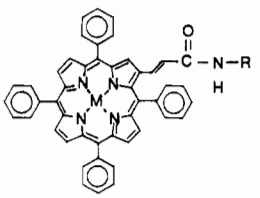

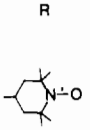

R	M	isomer	
	Cu	trans	I
	Cu	cis	II
	VO	cis	III
	Ag	trans	IV
	Ag	cis	V
	Cu	trans	VI
	Cu	cis	VII

have been found to agree well with those observed in rigid media.[3-5] It can be anticipated that molecular flexibility can

* To whom correspondence should be addressed at the University of Denver.

(1) Blankenship, R. E. *Acc. Chem. Res.* **1981**, *14*, 163–170. Klimov. V. V.; Krasnovskii, A. A. *Photosynthetica* **1981**, *15*, 592–609. Schulz, C. E.; Devaney, P. W.; Winkler, H.; Debrunner, P. G.; Doan, N.; Chiang, R.; Hager, L. P. *FEBS Lett.* **1979**, *103*, 102–105.

0020-1669/84/1323-1320$01.50/0